

# ESAT-6 Secretion-Independent Impact of ESX-1 Genes *espF* and *espG<sub>1</sub>* on Virulence of *Mycobacterium tuberculosis*

Daria Bottai,<sup>1,7</sup> Laleh Majlessi,<sup>2,5</sup> Roxane Simeone,<sup>1</sup> Wafa Frigui,<sup>1</sup> Christine Laurent,<sup>3,6</sup> Pascal Lenormand,<sup>3,6</sup> Jeffrey Chen,<sup>8</sup> Ida Rosenkrands,<sup>9</sup> Michel Huerre,<sup>4</sup> Claude Leclerc,<sup>2,5</sup> Stewart T. Cole,<sup>8</sup> and Roland Brosch<sup>1</sup>

<sup>1</sup>Institut Pasteur, UP Pathogénomique Mycobactérienne Intégrée; <sup>2</sup>Institut Pasteur, Unité de Régulation Immunitaire et Vaccinologie; <sup>3</sup>Institut Pasteur, Plate-Forme 3 Protéomique and Génopole; and <sup>4</sup>Institut Pasteur, Unité de Recherche et d'Expertise Histotechnologie et Pathologie; <sup>5</sup>Institut National de la Santé et de la Recherche Médicale, Unité 883; and <sup>6</sup>CNRS URA 2185, Paris, France; <sup>7</sup>Dipartimento di Patologia Sperimentale, Biotecnologie Mediche, Infettivologia ed Epidemiologia, University of Pisa, Pisa, Italy; <sup>8</sup>Global Health Institute, Ecole Polytechnique Fédérale de Lausanne, Lausanne, Switzerland; <sup>9</sup>Statens Serum Institut, Copenhagen, Denmark

**Background.** The pathogenesis of *Mycobacterium tuberculosis* largely depends on the secretion of the 6-kD early secreted antigenic target ESAT-6 (EsxA) and the 10-kD culture filtrate protein CFP-10 (EsxB) via the ESX-1/typeVII secretion system. Although gene products from the core RD1 region have been shown to be deeply implicated in this process, less is known about proteins encoded further upstream in the 5' region of the ESX-1 cluster, such as the ESX-1 secretion-associated proteins (Esp) EspF or EspG<sub>1</sub>.

**Methods.** To elucidate the role of EspF/G<sub>1</sub>, whose orthologs in *Mycobacterium marinum* and *Mycobacterium smegmatis* are reportedly involved in EsxA/B secretion, we constructed 3 *M. tuberculosis* knockout strains deleted for *espF*, *espG<sub>1</sub>* or the segment corresponding to the combined RD1<sup>bcg</sup>-RD1<sup>mic</sup> region of bacille Calmette-Guérin (BCG) and *Mycobacterium microti*, which also contains *espF* and *espG<sub>1</sub>*.

**Results.** Analysis of these strains revealed that, unlike observations with the model organisms *M. smegmatis* or *M. marinum*, disruption of *espF* and *espG<sub>1</sub>* in *M. tuberculosis* did not impact the secretion and T cell recognition of EsxA/B but still caused severe attenuation.

**Conclusions.** The separation of the 2 ESX-1-connected phenotypes (ie, EsxA/B secretion and virulence) indicates that EsxA/B secretion is not the only readout for a functional ESX-1 system and suggests that other processes involving EspF/G<sub>1</sub> also play important roles in ESX-1-mediated pathogenicity.

Full virulence of *Mycobacterium tuberculosis* relies on the secretion of the 6-kD early secreted antigenic target ESAT-6 (EsxA) and its protein partner, the 10-kD culture filtrate protein CFP-10 (EsxB) via the ESX-1/type VII secretion system [1, 2], which is encoded in the ESX-1 genomic locus close to the origin of replication [3]. Partially overlapping sections of this ESX-1 cluster are

missing from the genomes of the attenuated tubercle bacilli *Mycobacterium bovis* bacille Calmette-Guérin (BCG) and the vole bacillus *Mycobacterium microti*, due to independent deletion events that resulted in the loss of the region of difference 1 (RD1<sup>bcg</sup>) [4] and RD1<sup>mic</sup> [5], respectively. The study of RD1 genes in an *M. tuberculosis* genetic background has been enabled by the construction of an *M. tuberculosis* Δ RD1 strain (*Mtb*ΔRD1) that lacks the same 9.5-kb region as BCG. It was found that *Mtb*ΔRD1 mutants were attenuated in mice [6, 7], although in long-term infection studies, *Mtb*ΔRD1 was more virulent than BCG [8], which harbors additional attenuating mutations [9]. *Mtb*ΔRD1 was also useful for complementation studies identifying residues in EsxA required for the full virulence of *M. tuberculosis* [10].

Received 5 May 2010; accepted 8 July 2010.

Potential conflicts of interest: none reported.

Presented in part: ECCMID, Vienna, Austria, 10-13 April 2010.

Reprints or correspondence: Roland Brosch PhD, Institut Pasteur, 25 Rue du Dr Broux, 75724 Paris Cedex 15, France (roland.brosch@pasteur.fr).

**The Journal of Infectious Diseases** 2010;1155-64

© The Author 2010. Published by Oxford University Press on behalf of the Infectious Diseases Society of America. All rights reserved. For Permissions, please e-mail: journals.permissions@oup.com

1537-6613/2010/8-0001\$15.00

DOI: 10.1093/infdis/jiq089

However, *Mtb*ΔRD1 is not suitable for the study of the genomic locus *rv3865-66* from the 5' region of the ESX-1 cluster that encodes genes *espF* and *espG<sub>1</sub>* [11] and seems to be required for increased virulence of *M. microti*::RD1 strains [12]. In order to characterize *espF* and *espG<sub>1</sub>* in an authentic *M. tuberculosis* genetic background, we constructed 3 *M. tuberculosis* mutants in which either *espF*, or *espG<sub>1</sub>* was inactivated or from which a large segment, corresponding to the RD1<sup>mic</sup> and RD1<sup>bcg</sup> regions, was deleted. To establish the impact of *espF* and *espG<sub>1</sub>* in the function of the ESX-1 system, these knockout *M. tuberculosis* strains and their complemented derivatives were tested in various in vitro, ex vivo, and in vivo systems with particular emphasis on EsxA secretion and virulence.

## MATERIALS AND METHODS

### Plasmids, Bacterial Strains, Knockout Mutants and Complemented Strains

For the construction of knockout strains and complemented variants, we used plasmid pPR27 [13] and integrating vector pRBxint [14], respectively. For cloning procedures and plasmid amplification, *Escherichia coli* DH10B (Invitrogen) was used, whereas all mycobacterial knockout mutants were based on *M. tuberculosis* H37Rv [3, 14].

*M. tuberculosis* knockout mutants were constructed by allelic exchange using the Ts/*sacB* method [13]. Polymerase chain reaction (PCR) amplicons of genes and flanking regions (Table S1) and/or the kanamycin cassette were digested with appropriate endonucleases and cloned into *Bam*HI-*Not*I-digested pPR27. The resulting constructs, pPR-*espF*::Km, pPR-*espG<sub>1</sub>*::Km, and pPR-ΔΔ::Km, were sequenced and used for allelic replacement as described elsewhere [13]. For complementation, *espF*, *espG<sub>1</sub>*, or *espF-espH* fragments were cloned into pRBxint under the *dnaK* promoter [14]. Resulting plasmids pExint-*espF*, pExint-*espG<sub>1</sub>*, and/or pExint-*espF-espH* were electroporated into mutants and transformants selected after 4 weeks.

### RNA-Extraction, 5' -RACE, DNA-Extraction and Southern Analysis

RNA was extracted from bacteria in exponential-phase growth as described elsewhere [12] and used for rapid amplification of cDNA ends (RACE) and reverse-transcription PCR (Table S1), in accordance with the manufacturer's instructions (Roche).

Mycobacterial genomic DNA was extracted using standard protocols [5, 15]. To confirm allelic exchange, genomic DNAs from *Mtb*Δ*espF*, *Mtb*Δ*espG<sub>1</sub>*, or *Mtb*ΔΔRD1 were cleaved with *Pvu*II or *Afl*III and subjected to gel electrophoresis (*Mtb*Δ*espF* and *Mtb*Δ*espG<sub>1</sub>*) or pulsed-field gel-electrophoresis (*Mtb*ΔΔRD1). DNAs were blotted to Hybond-C nitrocellulose and hybridized with <sup>32</sup>P-labeled PCR fragments (Table S1) [5].

### Recombinant Protein Purification and Production of EspF/EspG1 Antisera

The *espF* and *espG<sub>1</sub>* coding sequenced were PCR amplified and cloned into pIVEX vectors (Roche). Recombinant EspF-6His and EspG<sub>1</sub>-6His were expressed in *E.coli* BL21 and purified using Ni<sup>2+</sup>-NTA affinity columns. Purified proteins were used for animal immunization. Similarly, the C-terminal part of EspA was expressed, purified, and used for raising polyclonal antibodies.

### Sample Preparation, Immunoblotting and 2D Electrophoresis

Preparation of mycobacterial protein extracts was performed as described elsewhere [12]. Immunoblotting was performed with mouse anti-EsxA (Hyb 76-8; Antibodyshop), mouse anti-GroEL2 monoclonal antibody (CSU), rat anti-EspG<sub>1</sub>-, or rabbit anti-PPE68 serum.

For 2D electrophoresis, culture filtrates from *M. tuberculosis* strains were concentrated in presence of ethylenediaminetetraacetic acid free protease inhibitor (Roche). Proteins were desalted and concentrated using the ReadyPrep 2-D Cleanup kit (BIO-RAD) and resuspended in 2D buffer (urea, 7M; thio urea, 2M; 4% CHAPS; 2% Triton X-100; 50 mM of DTT; pH4-7 ampholytes (2%). 2D gel electrophoresis was performed using pH 4–7-immobilized gradient strips for the first dimension and 15% sodium dodecyl sulfate–polyacrylamide gel electrophoresis (SDS-PAGE) for separation in the second dimension. Selected spots, such as EsxA/B, were confirmed by mass spectrometry.

### Splenocyte T cell Response Assays

C57BL/6 (H-2<sup>b</sup>) mice were injected subcutaneously with 10<sup>6</sup> colony-forming units (CFU) of H37Rv wild-type (WT) or mutants as described elsewhere [16, 17]. Two weeks after immunization, splenocytes were cultured (10<sup>6</sup> cells/well) for 72 h together with recombinant proteins/peptides, followed by quantification of the interferon (IFN)–γ level in culture supernatants using a sandwich enzyme-linked immunosorbent assay with AN-18 and biotin-conjugated R4-6A2 monoclonal antibodies.

### Ex vivo Virulence Analysis

Bone marrow-derived macrophages (BMDMs) and alveolar epithelial A549 cells were obtained, cultured, and infected as described elsewhere [12]. BMDMs and A549 cells were put in contact with bacterial suspensions at a multiplicity of infection of 1:1. At 4 h and at 4 and 7 days after infection, cells were lysed using .1% Triton X-100 in PBS and the number of intracellular bacteria was determined by plating serial dilutions of cell lysates.

### In vivo Virulence Analysis

Six-week-old C57BL/6 (H-2<sup>b</sup>) mice (Charles River) were infected via the aerosol route, as described elsewhere [12], using a suspension containing 5 × 10<sup>6</sup> CFU/mL to obtain an inhaled dose of ~100 CFU/lungs. Mice were killed 15 or 30 days after infection. Lungs and spleens were recovered and used for

determination of CFU counts and for histological examination, as described elsewhere [12, 17]. Experiments were undertaken in accordance with approved ethics guidelines, protocol No. 03-129.

## RESULTS

### Genetic Characterization, Inactivation and Complementation of the *espF/espG<sub>1</sub>* Locus in *M. tuberculosis*.

The genes *espF* and *espG<sub>1</sub>* are situated in the 5' region of the ESX-1 locus (Figure 1A). Analysis of the transcripts by RT-PCR using different combinations of primers specific for *espF* and *espG<sub>1</sub>* or their flanking genes showed that the 2 genes were co-transcribed and formed a transcriptional unit independent from the upstream gene *espE* and the downstream gene *espH* (Figure 1D). These results were confirmed by mapping the 5' ends of transcripts using 5' RACE, which identified independent *espE*- and *espF*-specific transcripts, starting 61 and 19 bases upstream of the start codons, respectively (Figures 1E–F).

To investigate the implication of *espF* and *espG<sub>1</sub>* in the ESX-1 secretion system, we constructed individual *M. tuberculosis* KO mutants (Figure 1B) that were complemented using integrating plasmids pExint-*espF*, pExint-*espG<sub>1</sub>*, or pExint-*espF-espH*. Quantitative RT-PCR (qRT-PCR) revealed that expression of *espH* was similar to WT in both KO mutants (Figure 1G), confirming the transcriptional separation of *espH* from *espF/G<sub>1</sub>*. Furthermore, qRT-PCR identified potential polar effects caused by the disruption of *espF* on *espG<sub>1</sub>* expression. Indeed, the level of expression of *espG<sub>1</sub>* in *MtbΔespF* was very low and remained low even after complementation with pExint-*espF*, wherein *espF* is under the control of the *dnaK* promoter. Higher levels of expression of *espG<sub>1</sub>* in the *MtbΔespF* genetic background were only obtained by complementation with pExint-*espF-espH* that included *espF* and *espG<sub>1</sub>*, as well as the unrelated *espH* gene (Figure 1G). Thus, only mutants complemented with the latter construct were used for subsequent studies.

To characterize the 5' region of the ESX-1 locus, we constructed an *M. tuberculosis* ESX-1 deletion strain lacking a genomic segment of almost 20 kb, corresponding to the RD1 regions absent from *M. microti* (RD1<sup>mic</sup>) and BCG (RD1<sup>bcg</sup>), which was named *MtbΔΔRD1* to reflect the absence of the 2 overlapping RD1 regions. This deletion mutant lacked the 5' and the core regions encoding the ESX-1 system (Figure 1). Complementation of *MtbΔΔRD1* was obtained with the cosmid pRD1-2F9 that was previously used to functionally complement BCG and *M. microti* [16, 18].

### Inactivation of *espF* or *espG<sub>1</sub>* Does Not Inhibit Secretion of ESX-1 Proteins in *M. tuberculosis*.

The ESX-1 locus of *M. tuberculosis* is highly conserved in *Mycobacterium marinum* and *Mycobacterium smegmatis* in gene content and gene order [19, 20]. Because previous

reports suggested that *espF* and *espG<sub>1</sub>* orthologs in *M. marinum* and *M. smegmatis* were involved in EsxA secretion [21, 22], it was of special interest to investigate whether *M. tuberculosis espF* and *espG<sub>1</sub>* KO mutants displayed a defect in ESX-1-related secretion.

EsxA was detected in the culture filtrates of *MtbΔespF*, *MtbΔespG<sub>1</sub>* and the WT control, whereas no EsxA was detected for *MtbΔΔRD1* (Figure 2A). Lysis controls using antibodies against GroEL2 or PPE68 indicated that the samples were not contaminated with cytosolic or membrane-associated proteins. Together, these results strongly suggest that, in *M. tuberculosis*, the inactivation of *espF* or *espG<sub>1</sub>* does not inhibit the secretion of EsxA.

Because secretion of EspA (Rv3616c) was reported to be EsxA dependent [23], the presence of EspA in the supernatants of the mutants was tested using antibodies raised against the C-terminal part of EspA. A weak but specific band of 40 kD was detected in the supernatants of *MtbΔespF*, *MtbΔespG<sub>1</sub>*, and complemented strains. Although more EspA was observed for the WT, the finding that complementation of the mutants did not increase the amount of EspA suggests that *espF* and *espG<sub>1</sub>* are not directly involved in this process.

We also tested polyclonal anti-EspF and anti-EspG<sub>1</sub> antibodies. For EspF, no specific protein detection was observed among the WT and mutants under the conditions used (data not shown), although qRT-PCR results suggested expression of *espF* (Figure 1G). In contrast, anti-EspG<sub>1</sub> antibodies revealed a specific band of 30 kD in WT and complemented strains that was absent from the KO mutants (Figure 2A and 2C). Although the absence of EspG<sub>1</sub> from both KO mutants confirms the aforementioned transcriptional link between *espF* and *espG<sub>1</sub>*, the localization of EspG<sub>1</sub> in the membrane and cell-wall fractions, together with the absence from culture filtrate, indicates that EspG<sub>1</sub> is a component of the mycobacterial cell envelope. Whereas topology analysis using MEMSAT3 [24] did not identify a signal peptide in EspG<sub>1</sub>, a potential transmembrane helix is predicted at lower confidence scores (data not shown).

Finally, screening of total lysates from KO mutants with anti-PPE68 antibodies revealed the presence of this RD1-encoded PPE protein in preparations of all strains except *MtbΔΔRD1* (Figure 2A). However, more detailed analysis showed that the amounts of PPE68 in the cell envelope preparations from *MtbΔespF* and *MtbΔespG<sub>1</sub>* were repeatedly lower than those detected in the complemented and the WT strains, suggesting a functional link between the *espF/espG<sub>1</sub>* locus and *ppe68* gene expression or PPE68 protein stability (Figure 2C).

### Posttranslational Modification of EsxA is Unaffected in *espF* and *espG<sub>1</sub>* Mutant Strains

Previous studies using 2D gels of culture filtrate proteins of *M. tuberculosis* suggested that EsxA is present in these preparations in different forms that carry posttranslational modifications,

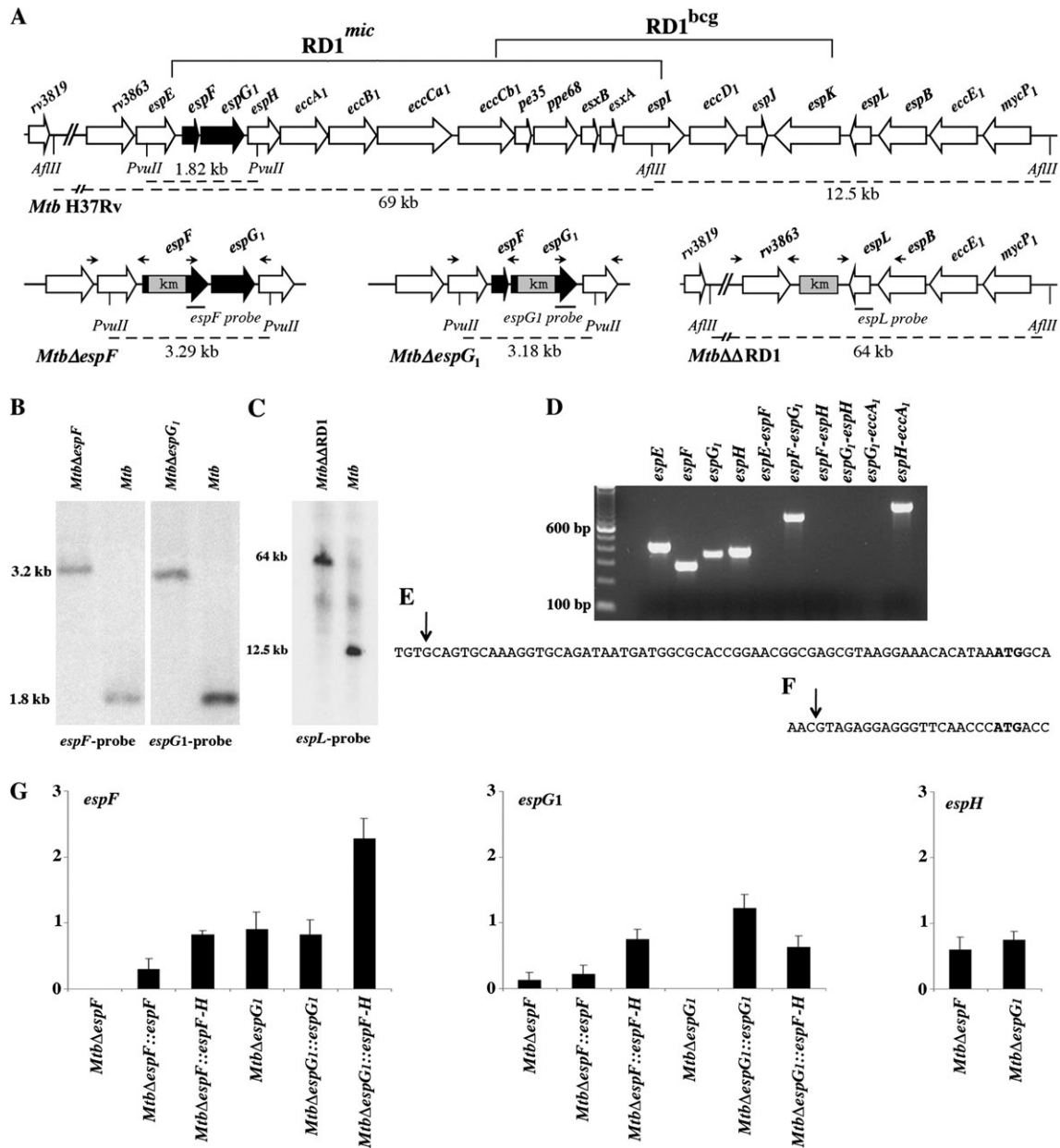


**Figure 1.** Characterization of *Mycobacterium tuberculosis* mutants. *A*, Genomic organization of RD1<sup>mic</sup>-RD1<sup>bcg</sup> region in *M. tuberculosis* H37Rv and KO strains. *Arrows*, primers used for construction of mutants. *B*, Southern blot analysis of genomic DNA from *MtbΔespF*, *MtbΔespG1*, and *M. tuberculosis* H37Rv WT digested by *PvuII* and probed with an *espF*- or *espG1*-specific probe. *C*, Pulsed-field gel electrophoresis (Ramp, 1–18 s; 22 h at 6 V/cm) and Southern blot of *AflIII*-digested genomic DNA from *MtbΔΔRD1* and WT strains probed with an *espL*-specific probe. Note that the deletion of the RD1<sup>mic</sup>-RD1<sup>bcg</sup> region is accompanied by the loss of an *AflIII* restriction site, resulting in an *espL*-containing hybridization fragment that is larger than that obtained from the WT strain. *D*, Analysis of the *M. tuberculosis* *espF*-*espG1* locus by reverse-transcription polymerase chain reaction (RT-PCR) of RNA from *M. tuberculosis* H37Rv using various combinations of primers specific for *espF*, *espG1*, and their flanking genes. *E* and *F*, DNA sequences of the regions upstream of the *espE* (*E*) and *espF* (*F*) genes. 5' ends of transcripts, mapped by 5' RACE, are indicated by arrows. Translational start sites are in boldface font. *G*, Expression levels of the genes *espF*, *espG1*, and *espH* in cultures of *MtbΔespF*, *MtbΔespG1*, and corresponding complemented strains evaluated by quantitative RT-PCR. The expression level of each gene in each strain is reported as the ratio between the mutant and *M. tuberculosis* H37Rv WT, used as reference. For each strain, values were normalized to the level of 16S rRNA expression, which exists as a single copy in *M. tuberculosis*. Primer and probe sequences of genes *espF*, *espG1*, *espH*, and 16S rRNA are listed in Table S1. *Km*, kanamycin resistance gene.

such as acetylation of the N-terminal threonine residue [25]. Thus, we tested whether inactivation of EspF and/or EspG<sub>1</sub> had any visible effect on 2D electrophoresis patterns of EsxA, but no

differences between the WT and the 2 deletion mutants were found (Figure 2D). As expected, no EsxA/B was detected in the culture filtrate of *MtbΔΔRD1*.

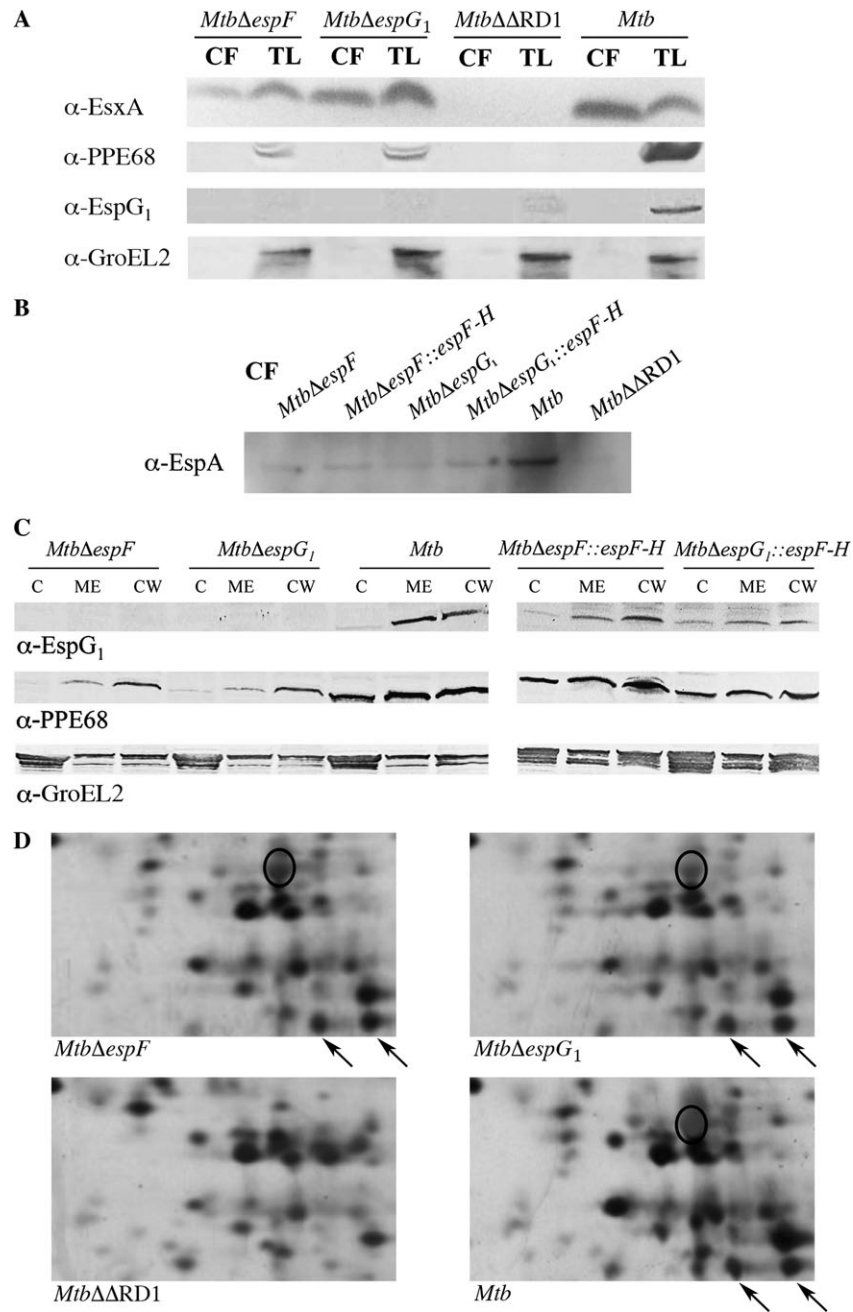


**Figure 2.** In vitro expression and secretion of ESX-1 proteins in *MtbΔespF*, *MtbΔespG<sub>1</sub>*, and *MtbΔΔRD1* strains. Culture filtrates (CFs) were obtained as supernatants of bacterial cultures grown in Sauton medium for 4–6 days, recovered by centrifugation, and concentrated using filters with a 3-kD cutoff. Total lysates (TLs) were obtained by shaking bacterial pellets with 106- $\mu$ m acid-washed glass beads and centrifugation at  $2300 \times g$  for 30 min. Cell wall (CW), cytosolic (C) membrane (ME) fractions were prepared from total lysates by 45-min centrifugation at  $17,500 \times g$  (CW), followed by ultracentrifugation at  $3,50,000 \times g$  rpm for 90 min (C and ME). Protein concentrations were determined and normalized using a BioRad protein assay before sodium-dodecyl-sulfate-polyacrylamide gel-electrophoresis (SDS - PAGE). *A*, Fifteen micrograms of CF or TL were subjected to SDS - PAGE and tested by Western blotting using monoclonal anti-EsxA antibodies Hyb 76-8a, anti-EspG<sub>1</sub> rat polyclonal serum, polyclonal rabbit anti-EspA, or anti-PPE68 serum. Mouse anti-GroEL2 antibodies were used for lysis controls. *B*, Immunoblot showing bands in the size range of 40 kD obtained from CF proteins using anti-EspA antibodies. *C*, Forty micrograms of C, ME, and CW fractions from *MtbΔespF*, *MtbΔespG<sub>1</sub>* and their complemented variants as well as from *M. tuberculosis* H37Rv WT were tested by Western blotting with anti-EspG<sub>1</sub> rat polyclonal serum, anti-PPE68 rabbit polyclonal serum, or anti-GroEL2 antibodies. Note that the presence of various bands with slightly different molecular weight for GroEL2 might have been enhanced by the additional centrifugation steps used for preparing the subcellular fractions. *D*, Two-dimensional analysis of CF from *MtbΔespF*, *MtbΔespG<sub>1</sub>*, *MtbΔΔRD1*, and *M. tuberculosis* H37Rv WT focused on EsxA/B spots. Eighty-five micrograms of CF proteins were separated by isofocusing using a pH 4–7 gradient and 15% SDS - PAGE, in the first and second dimension, respectively. Protein detection was performed by silver staining. EsxA and EsxB spots are indicated by arrows and circles, respectively. For simplicity, only the regions of the gels containing EsxA and EsxB spots are shown.

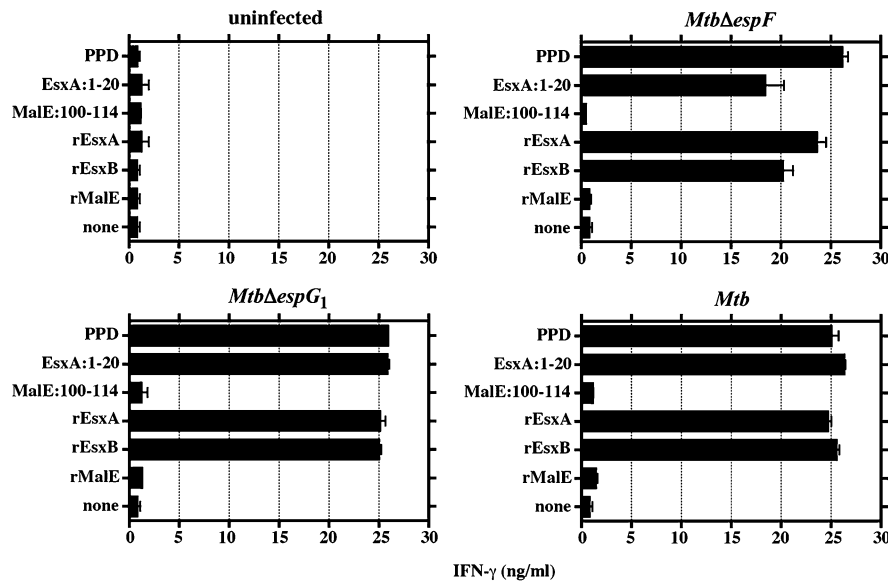


**Figure 3.** EsxA- and EsxB-specific T cell responses induced by *MtbΔespF* and *MtbΔespG1* strains 2 weeks after mouse immunization. Splenocytes were cultured for 72 h with 4 μg/mL recombinant EsxA or EsxB or with 1 μg/mL EsxA:1–20 synthetic peptide. As positive and negative controls, interferon-γ production was also evaluated in response to 5 μg/mL purified-protein derivative (PPD) and to recombinant Mal-E protein or MalE:100–114 peptide. The data are representative of 2 independent experiments.

### Immune Recognition of EsxA Is Not Affected by *espF/espG1* Disruption

The ability to stimulate EsxA/B-specific T cells in mice requires secretion of these antigens [26, 27]. When *MtbΔespF*, *MtbΔespG1*, and WT strains were tested for their potential to induce specific T cell responses against ESX-1 antigens, all 3 strains induced high and comparable amounts of IFN-γ production after stimulation with EsxA or EsxB (Figure 3). Together with the finding that all strains induced IFN-γ production in response to purified protein derivative but not the Mal-E controls, the results validate the ability of *MtbΔespF* and *MtbΔespG1* to secrete EsxA/B under in vivo conditions.

### Virulence Determination of Strains

As part of an initial virulence test, *MtbΔespF*, *MtbΔespG1*, or *MtbΔARD1* mutants were subjected to ex vivo growth analysis in BMDMs and in a A549 type II pneumocytic cell line. *MtbΔespF* and *MtbΔespG1* mutants were engulfed by both cell types equally well as the control (Figure 4A). However, both mutants showed reduced growth in BMDMs (Figure 4B), whereas the growth characteristics in pneumocytes were similar to those in the WT control (Figure 4C). The most severe attenuation was observed for *MtbΔARD1*, which was engulfed less efficiently than the control and which also showed significant growth attenuation in both cell types (Figure 4B and 4C).

The impact of *espF* and *espG1* inactivation on virulence was then assessed by comparing the behavior of *MtbΔespF*, *MtbΔespG1*, and *MtbΔARD1* in aerosol-infected mice. Whereas the WT control replicated extensively in the organs, *MtbΔespF*

and *MtbΔespG1* showed attenuated phenotypes. At day 30 after infection, a 3- and 2-log<sub>10</sub> difference was observed in the number of CFU recovered from the lungs and spleen of mice infected with *MtbΔespG1*, compared with the WT control. Similarly, for *MtbΔespF*, a 4- and 3-log<sub>10</sub> reduction in the number of CFU recovered from the lungs and spleen, respectively, was observed (Figure 5A and 5B). The attenuation of the mutants was also confirmed by histological analyses, which identified no (or only minimal) lesions in sections of lungs from mice infected with *MtbΔespF* and *MtbΔespG1*, whereas multiple and extended granulomas were detected in lungs from WT-infected mice (Figure 6). Complementation of *MtbΔespF* and *MtbΔespG1* with the *espF-espH* region increased the virulence of the strains, although it did not restore the virulence to the level of the WT (Figure 5A and 5B).

In good agreement with results from the infection of macrophages and pneumocytes, *MtbΔARD1* was most strongly attenuated also in the mouse infection model. Deletion of almost all ESX-1 genes resulted in a 4-log<sub>10</sub> reduction of the number of CFU recovered from lungs, compared with for the control, 30 days after infection and in no colonies recovered from the spleen (Figure 5B). Furthermore, histological analysis of lung sections revealed predominantly normal lung tissue, with no granuloma or lesions (Figure 6), thus confirming the strong attenuation of *MtbΔARD1*.

These results prompted us to evaluate the virulence of *MtbΔARD1* compared with that of *MtbΔRD1*, which lacks only the RD1 core region [6], and with that of BCG. As depicted in Figure 5C–5D, in this final virulence test, *MtbΔARD1* again

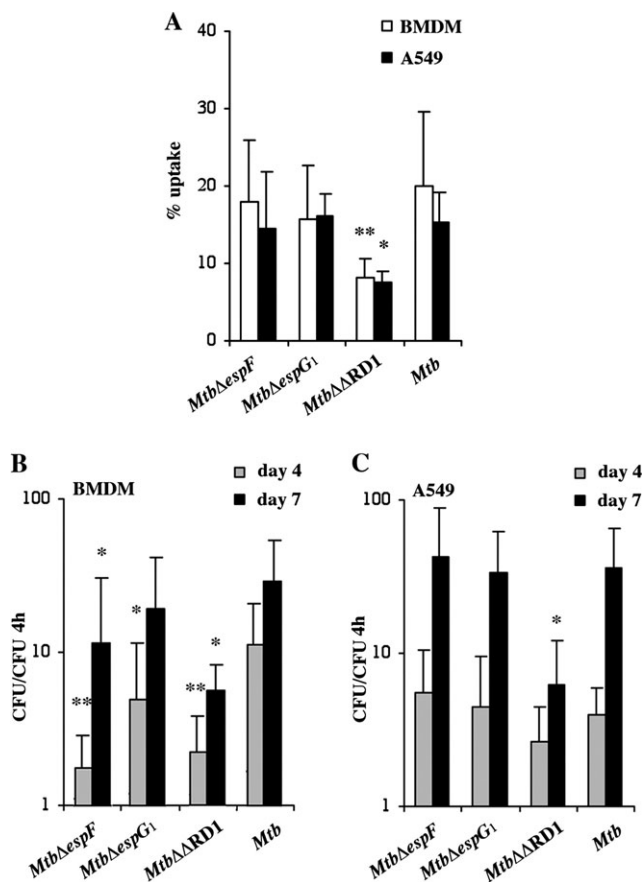


**Figure 4.** Intracellular growth of *MtbΔespF*, *MtbΔespG<sub>1</sub>*, and *MtbΔΔRD1* strains in bone marrow–derived macrophages (BMDMs) and A549 cells. *A*, Quantification of bacterial uptake 4 h after infection of murine macrophages (■) and A549 cells (□) with *MtbΔespF*, *MtbΔespG<sub>1</sub>*, and *MtbΔΔRD1* strains using a multiplicity of infection (MOI) of 1:1 (bacteria:cell). *B* and *C*, Colony-forming unit (CFU) ratio values (number of CFUs at days 4 and 7 relative to the number of CFUs at 4 h) in BMDMs (*B*) and A549 cells (*C*). The figures show the means and the standard deviations of percentages of uptake or CFU ratio values obtained in 3 independent experiments, each performed in quadruplicate. The significant difference in percentages of uptake or CFU ratio values between H37Rv and the mutant strains (*MtbΔespF*, *MtbΔespG<sub>1</sub>*, and *MtbΔΔRD1*) were determined by analysis of variance (one-way ANOVA test), followed by Bonferroni means comparison test. \**P* < .05. \*\**P* < .01.

showed very limited in vivo growth, with lower CFU counts in lungs and spleens than *MtbΔRD1*. It is noteworthy that the *MtbΔΔRD1*, unlike *MtbΔRD1*, scarcely disseminated to the spleen (Figure 5D). These findings, which confirm and extend observations described for BCG and *MtbΔRD1* [8], suggest that the level of attenuation resulting from the deletion of the RD1 core region can still be enhanced by additional mutations that affect the in vivo growth of tubercle bacilli [9, 28]. Simultaneous deletion of the genes located in the 5' end of the ESX-1 cluster in addition to the RD1 core region thus represents a novel combination resulting in profound attenuation of *M. tuberculosis*.

## DISCUSSION

It is well known that several proteins of the ESX-1 secretion system encoded in the 9.5-kb RD1 core region, which is present in *M. tuberculosis* but absent from the attenuated BCG vaccine strain, play important roles in mycobacterial virulence [6, 7, 18, 29, 30]. In contrast, much less information is available on the genes situated further upstream in the extended RD1 region of *M. tuberculosis*. Thus, in this study, we focused on 2 genes, recently named *espF* and *espG<sub>1</sub>* [11], that are both encoded in the extended RD1 region of *M. tuberculosis* and for which preliminary *M. microti*-derived data suggested a potential involvement in virulence [12]. To experimentally address this issue, it was of utmost importance to construct individual *M. tuberculosis* KO mutants of genes *espF* and *espG<sub>1</sub>*, respectively, as well as a *M. tuberculosis* deletion mutant that lacks a 20-kb genomic segment spanning the genes upstream of the RD1 region in addition to the core RD1 locus. These mutants were not only of key importance for the present study but also represent excellent tools for further in-depth studies of the ESX-1 secretion apparatus of *M. tuberculosis*.

We show here that *espF* and *espG<sub>1</sub>* from *M. tuberculosis* form an operon that is transcribed independently from the neighboring genes *espE* and *espH*. Such a genomic organization is in agreement with the downstream effects on gene expression for *espG<sub>1</sub>*, which were initially observed in qRT-PCR analyses on attempting to complement the *MtbΔespF* mutant with an *espF*-expressing plasmid and which prompted us to complement the mutants with a plasmid including *espG<sub>1</sub>* in addition to *espF*.

With use of antibodies against EspF, no specific protein detection was observed, possibly because of low stability of EspF under the conditions in the study. EspF was previously identified in proteomic studies as a secreted protein of *M. tuberculosis* [31] and, more recently, as an ESX-1–dependent secreted protein in *M. marinum* [32]. However, in the same study, only very small amounts of EspF were identified for *M. tuberculosis*. This finding is in agreement with our data and suggests that the expression kinetics, stability, and/or function of EspF may not be the same for different mycobacterial species in spite of the primary sequence similarities.

A comparable situation is observed for EspG<sub>1</sub>. Different research groups working on the ESX-1 system of *M. marinum* and/or *M. smegmatis* have reported that EspG<sub>1Mm</sub> transposon or EspG<sub>1Ms</sub> KO mutants showed a defect in EsxA/B secretion [21, 33]. Conversely, in *M. tuberculosis*, we find that inactivation of EspG<sub>1Mt</sub> has no obvious effect on secretion of EsxA. As shown in the numerous SDS-PAGE experiments performed during this study, the supernatants from *MtbΔespF* and *MtbΔespG<sub>1</sub>* mutants always contained large amounts of EsxA and exhibited a very similar 2D profile to WT *M. tuberculosis*. These findings indeed suggest that, in *M. tuberculosis*, EspF and EspG<sub>1</sub> are not directly involved in EsxA secretion or posttranslational modifications of

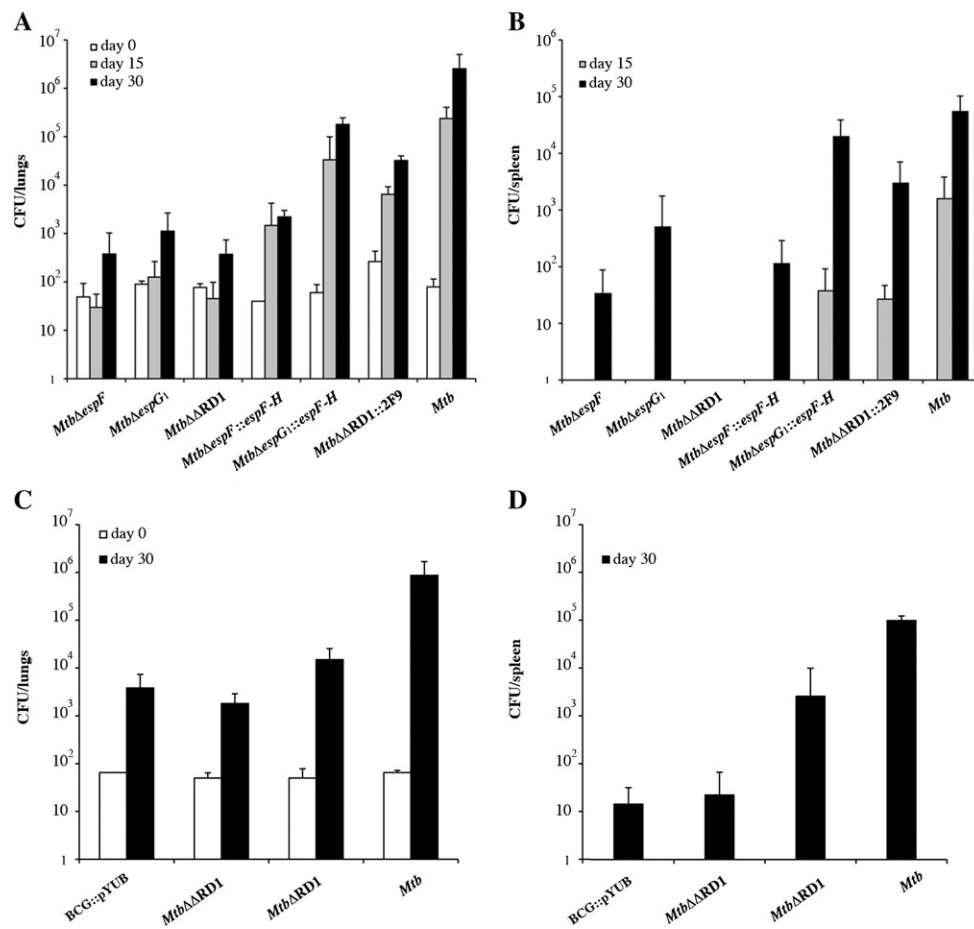


**Figure 5.** Analysis of the virulence of different strains in an aerosol infection model using C57BL/6 mice. The number of colony-forming units (CFUs) of *MtbΔespF*, *MtbΔespG<sub>1</sub>*, *MtbΔARD1* or their complemented derivatives, as well as of wild-type (WT) *Mycobacterium tuberculosis* H37Rv in the lungs (A) and spleens (B) of C57BL/6 mice 15 and 30 days after infection, compared with the number of CFUs in lungs at day 0. The figure shows the means and standard deviations of CFU values obtained in 2 independent experiments, each performed with 4–5 mice per group. The CFU values are also shown for bacille Calmette-Guérin (BCG), *MtbΔARD1*, *MtbΔARD1*, and WT *M. tuberculosis* H37Rv strains in the lungs (C) and spleens (D) of C57BL/6 mice 30 days after infection, compared with the CFU values in lungs at day 0.

EsxA. This is further confirmed by the fact that the EspF and EspG<sub>1</sub> mutants also induced strong EsxA/B-specific T cell responses in an antigen-specific IFN-γ secretion assay, representing a sensitive and reliable readout system of EsxA secretion in *M. tuberculosis* [26, 27]. We cannot yet exclude the possibility that there is a potential overlap of function between EspF and the chromosomally unlinked ESX-1 protein EspC (Rv3615c; 67% amino acid similarity as determined by FASTA alignment) that might contribute to the continued EsxA secretion in the *MtbΔespF* mutant. However, even if that were the case, such an effect does not alleviate the attenuation of the mutant.

From these data, we can conclude that the attenuation of the *M. tuberculosis* EspF and EspG<sub>1</sub> mutants is not caused by the lack of EsxA secretion but, rather, by the interruption of another, yet-unknown function of the ESX-1 system. One of the apparent possibilities might relate to the interaction of EspF and/or EspG<sub>1</sub> with other proteins. It was, for example, reported that EspF shows protein-protein interaction with the AAA+ ATPase EccA<sub>1</sub> [32],

although the biological consequences of this interaction are not known. For EspG<sub>1</sub> a strong and specific interaction with the PPE68 protein of the ESX-1 system was reported elsewhere [34]. This finding is in agreement with the observation that EspF and EspG<sub>1</sub> mutants show substantially lower amounts of PPE68 in their cell lysates (Figure 2C). However, the role of PPE68 in the ESX-1 system remains unclear. Although *ppe68* (*rv3873*) was listed among the genes that were required for full virulence of *M. tuberculosis* revealed by a genome-wide transposon site hybridization screen [35], interruption or truncation of the C-terminal part of the PPE68 protein did not result in the attenuation of the recombinant strains [12, 36]. Future studies involving unmarked *ppe68* KO strains may elucidate this aspect.

Finally, it might be argued that the reason for EspF and EspG<sub>1</sub> not being implicated in the secretion of EsxA/B in *M. tuberculosis* is that EspF and EspG<sub>1</sub> were simply not part of the ESX-1 system. Although we cannot exclude with certainty such a scenario, several points suggest that EspF and EspG<sub>1</sub> do play a role

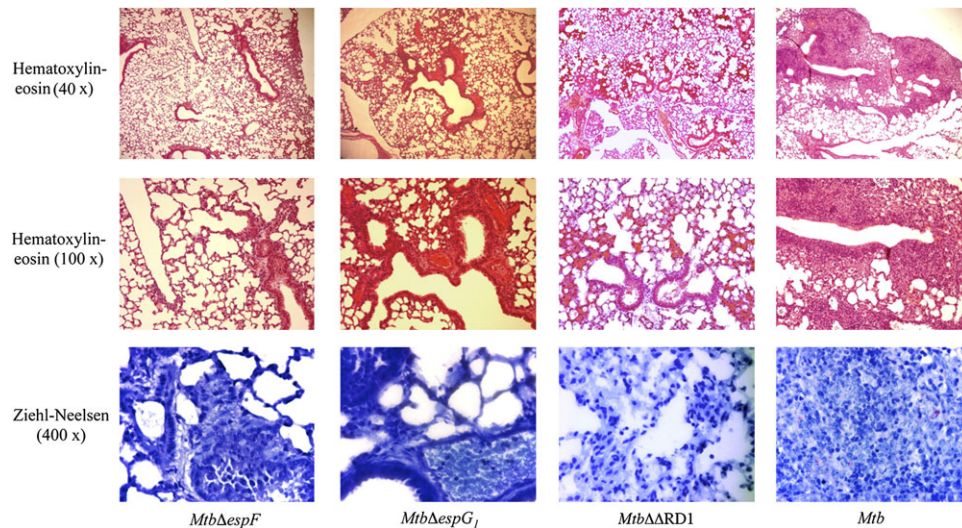


**Figure 6.** Lung histopathology subsequent to low-dose aerosol infection of C57BL/6 mice with *MtbΔespF*, *MtbΔespG<sub>1</sub>*, *MtbΔARD1*, and *Mycobacterium tuberculosis* H37Rv control strains. Thirty days after infection, lungs were removed, fixed in 10% buffered formalin, and stained with hematoxylin-eosin or Ziehl-Neelsen stain. The figure shows histological sections of a representative mouse for each group of infected mice. Original magnification,  $\times 40$  and  $\times 100$  for hematoxylin-eosin stains and  $\times 400$  for Ziehl-Neelsen stains.

in the ESX-1 systems of *M. tuberculosis*. First, by looking at the genome arrangement, *espF* and *espG<sub>1</sub>* are clearly located within the ESX-1 cluster. *EspF* is also 67% similar to *EspC*, which is functionally linked with ESX-1 [37]. Furthermore, *M. tuberculosis* contains a total of 5 ESX/type VII systems [2, 3, 19, 38–40] that, apart from ESX-conserved components PE/PPE- and *Esx*-proteins [11], also contain ESX-associated proteins, such as the ESX-1 secretion-associated proteins *Esp*s [11, 23, 37]. *EspG<sub>1</sub>* belongs to the latter group, but in contrast to other *Esp* proteins that share no homologues in the *M. tuberculosis* genome, related *EspG<sub>2</sub>/G<sub>3</sub>* proteins are present in ESX-2 and ESX-3 systems [11]. Because ESX clusters are considered to have evolved by duplication and subsequent diversification [19], the presence of *espG* genes in different ESX loci suggests that *EspG* variants were already part of ESX clusters in earlier steps of mycobacterial evolution, further underlining the close link between *espG<sub>1</sub>* and the ESX-1 system. The separation of the 2 ESX-1-related phenotypes (*EsxA/B* secretion and virulence) reported here thus strongly suggests that *EsxA/B* secretion is not the only essential function of the ESX-1 system contributing to host-pathogen interaction. These insights are of central interest for the elucidation of the function of the ESX-1 system of *M. tuberculosis* and suggest that, despite the similar genetic organization of ESX-1 loci in various mycobacterial species, substantial differences in the secretion machinery might exist that have evolved during the adaptation of different mycobacterial species to their respective ecological niches.

### Supplementary Data

Supplementary data are available at [http://www.oxfordjournals.org/our\\_journals/jid/online](http://www.oxfordjournals.org/our_journals/jid/online).

### Funding

This work was supported in part by the Swiss National Science Foundation (31003A-125061) and has received funding from the European Community's Seventh Framework Programme ([FP7/2007-2013]) under grant agreement n°201762.

### Acknowledgments

We are grateful to Priscille Brodin for help in the initial phase of the project, Marien DeJonge for help with expression and purification of *EspF* and *EspG<sub>1</sub>* proteins used for antibody production, and Eddie Maranghi for expert assistance in animal care. We also thank Marcella Simsova and Peter Sebo (Czech Academy of Sciences) for providing recombinant *EsxA/B* for splenocyte T cell response assays. Antibodies against GroEL2 were received as part of National Institutes of Health, National Institute of Allergy and Infectious Diseases contract entitled “Tuberculosis Vaccine Testing and Research Materials,” awarded to Colorado State University.

### References

1. Simeone R, Bottai D, Brosch R. ESX/type VII secretion systems and their role in host-pathogen interaction. *Curr Opin Microbiol* **2009**; 12:4–10.
2. Abdallah A, Gey van Pittius N, Champion P, et al. Type VII secretion-mycobacteria show the way. *Nat Rev Microbiol* **2007**; 5:883–91.
3. Cole ST, Brosch R, Parkhill J, et al. Deciphering the biology of *Mycobacterium tuberculosis* from the complete genome sequence. *Nature* **1998**; 393:537–44.
4. Mahairas GG, Sabo PJ, Hickey MJ, Singh DC, Stover CK. Molecular analysis of genetic differences between *Mycobacterium bovis* BCG and virulent *M. bovis*. *J Bacteriol* **1996**; 178:1274–82.
5. Brodin P, Eiglmeier K, Marmiesse M, et al. Bacterial artificial chromosome-based comparative genomic analysis identifies *Mycobacterium microti* as a natural ESAT-6 deletion mutant. *Infect Immun* **2002**; 70:5568–78.
6. Hsu T, Hingley-Wilson SM, Chen B, et al. The primary mechanism of attenuation of bacillus Calmette-Guerin is a loss of secreted lytic function required for invasion of lung interstitial tissue. *Proc Natl Acad Sci U S A* **2003**; 100:12420–5.

7. Lewis KN, Liao R, Guinn KM, et al. Deletion of RD1 from *Mycobacterium tuberculosis* mimics bacille Calmette-Guerin attenuation. *J Infect Dis* **2003**; 187:117–23.
8. Sherman DR, Guinn KM, Hickey MJ, Mathur SK, Zakel KL, Smith S. *Mycobacterium tuberculosis* H37Rv: delta RD1 is more virulent than *M. bovis* bacille Calmette-Guerin in long-term murine infection. *J Infect Dis* **2004**; 190:123–6.
9. Brosch R, Gordon SV, Garnier T, et al. Genome plasticity of BCG and impact on vaccine efficacy. *Proc Natl Acad Sci U S A* **2007**; 104:5596–601.
10. Brodin P, de Jonge MI, Majlessi L, et al. Functional analysis of early secreted antigenic target-6, the dominant T-cell antigen of *Mycobacterium tuberculosis*, reveals key residues involved in secretion, complex formation, virulence, and immunogenicity. *J Biol Chem* **2005**; 280:33953–9.
11. Bitter W, Houben EN, Bottai D, et al. Systematic genetic nomenclature for type VII secretion systems. *PLoS Pathog* **2009**; 5:e1000507.
12. Brodin P, Majlessi L, Marsollier L, et al. Dissection of ESAT-6 system 1 of *Mycobacterium tuberculosis* and impact on immunogenicity and virulence. *Infect Immun* **2006**; 74:88–98.
13. Pelicic V, Jackson M, Reyrat JM, Jacobs WR Jr, Gicquel B, Guilhot C. Efficient allelic exchange and transposon mutagenesis in *Mycobacterium tuberculosis*. *Proc Natl Acad Sci U S A* **1997**; 94:10955–60.
14. Fernandez P, Saint-Joanis B, Barilone N, et al. The Ser/Thr protein kinase PknB is essential to sustain mycobacterial growth. *J Bacteriol* **2006**; 188:7778–84.
15. van Soolingen D, Hermans PWM, de Haas PEW, Soll DR, van Embden JDA. Occurrence and stability of insertion sequences in *Mycobacterium tuberculosis* complex strains: evaluation of an insertion sequence-dependent DNA polymorphism as a tool in the epidemiology of tuberculosis. *J Clin Microbiol* **1991**; 29:2578–86.
16. Brodin P, Majlessi L, Brosch R, et al. Enhanced protection against tuberculosis by vaccination with recombinant *Mycobacterium microti* vaccine that induces T cell immunity against region of difference 1 antigens. *J Infect Dis* **2004**; 190:115–22.
17. Majlessi L, Brodin P, Brosch R, et al. Influence of ESAT-6 secretion system 1 (RD1) of *Mycobacterium tuberculosis* on the interaction between mycobacteria and the host immune system. *J Immunol* **2005**; 174:3570–9.
18. Pym AS, Brodin P, Brosch R, Huerre M, Cole ST. Loss of RD1 contributed to the attenuation of the live tuberculosis vaccines *Mycobacterium bovis* BCG and *Mycobacterium microti*. *Mol Microbiol* **2002**; 46:709–17.
19. Gey Van Pittius NC, Gamielidien J, Hide W, Brown GD, Siezen RJ, Beyers AD. The ESAT-6 gene cluster of *Mycobacterium tuberculosis* and other high G+C Gram-positive bacteria. *Genome Biol* **2001**; 2:RESEARCH0044.
20. Marmiesse M, Brodin P, Buchrieser C, et al. Macro-array and bioinformatic analyses reveal mycobacterial ‘core’ genes, variation in the ESAT-6 gene family and new phylogenetic markers for the *Mycobacterium tuberculosis* complex. *Microbiology* **2004**; 150:483–496.
21. Gao LY, Guo S, McLaughlin B, Morisaki H, Engel JN, Brown EJ. A mycobacterial virulence gene cluster extending RD1 is required for cytolysis, bacterial spreading and ESAT-6 secretion. *Mol Microbiol* **2004**; 53:1677–93.
22. Flint JL, Kowalski JC, Karnati PK, Derbyshire KM. The RD1 virulence locus of *Mycobacterium tuberculosis* regulates DNA transfer in *Mycobacterium smegmatis*. *Proc Natl Acad Sci U S A* **2004**; 101:12598–603.
23. Fortune SM, Jaeger A, Sarracino DA, et al. Mutually dependent secretion of proteins required for mycobacterial virulence. *Proc Natl Acad Sci U S A* **2005**; 102:10676–81.
24. Jones DT. Improving accuracy transmembrane protein topology prediction using evolutionary information. *Bioinformatics* **2007**; 23:538–44.
25. Okkels LM, Muller EC, Schmid M, et al. CFP10 discriminates between nonacetylated and acetylated ESAT-6 of *Mycobacterium tuberculosis* by differential interaction. *Proteomics* **2004**; 4:2954–60.
26. Pym AS, Brodin P, Majlessi L, et al. Recombinant BCG exporting ESAT-6 confers enhanced protection against tuberculosis. *Nat Med* **2003**; 9:533–9.
27. Frigui W, Bottai D, Majlessi L, et al. Control of *M. tuberculosis* ESAT-6 secretion and specific T cell recognition by PhoP. *PLoS Pathog* **2008**; 4:e33.
28. Gordon SV, Bottai D, Simeone R, Stinear TP, Brosch R. Pathogenicity in the tubercle bacillus: molecular and evolutionary determinants. *Bioessays* **2009**; 31:378–88.
29. Guinn KI, Hickey MJ, Mathur SK, et al. Individual RD1-region genes are required for export of ESAT-6/CFP-10 and for virulence of *Mycobacterium tuberculosis*. *Mol Microbiol* **2004**; 51:359–70.
30. Stanley SA, Raghavan S, Hwang WW, Cox JS. Acute infection and macrophage subversion by *Mycobacterium tuberculosis* require a specialized secretion system. *Proc Natl Acad Sci U S A* **2003**; 100:13001–6.
31. Bahk YY, Kim SA, Kim JS, et al. Antigens secreted from *Mycobacterium tuberculosis*: identification by proteomics approach and test for diagnostic marker. *Proteomics* **2004**; 4:3299–307.
32. DiGiuseppe Champion PA, Champion MM, Manzanillo P, Cox JS. ESX-1 secreted virulence factors are recognized by multiple cytosolic AAA ATPases in pathogenic mycobacteria. *Mol Microbiol* **2009**; 73:950–62.
33. Converse SE, Cox JS. A protein secretion pathway critical for *Mycobacterium tuberculosis* virulence is conserved and functional in *Mycobacterium smegmatis*. *J Bacteriol* **2005**; 187:1238–45.
34. Teutschbein J, Schumann G, Mollmann U, Grabley S, Cole ST, Munder T. A protein linkage map of the ESAT-6 secretion system 1 (ESX-1) of *Mycobacterium tuberculosis*. *Microbiol Res* **2009**; 164:253–9.
35. Sassetti CM, Rubin EJ. Genetic requirements for mycobacterial survival during infection. *Proc Natl Acad Sci U S A* **2003**; 100:12989–94.
36. Demangel C, Brodin P, Cockle PJ, et al. Cell envelope protein PPE68 contributes to *Mycobacterium tuberculosis* RD1 immunogenicity independently of a 10-kilodalton culture filtrate protein and ESAT-6. *Infect Immun* **2004**; 72:2170–6.
37. MacGurn JA, Raghavan S, Stanley SA, Cox JS. A non-RD1 gene cluster is required for Snm secretion in *Mycobacterium tuberculosis*. *Mol Microbiol* **2005**; 57:1653–63.
38. Siegrist MS, Unnikrishnan M, McConnell MJ, et al. Mycobacterial Esx-3 is required for mycobactin-mediated iron acquisition. *Proc Natl Acad Sci U S A* **2009**; 106:18792–7.
39. Serafini A, Boldrin F, Palu G, Manganelli R. Characterization of a *Mycobacterium tuberculosis* ESX-3 conditional mutant: essentiality and rescue by iron and zinc. *J Bacteriol* **2009**; 191:6340–4.
40. Bottai D, Brosch R, Mycobacterial PE. PPE and ESX clusters: novel insights into the secretion of these most unusual protein families. *Mol Microbiol* **2009**; 73:325–8.